ISSN (Print) 1226-1750
ISSN (Online) 2233-6656
Journal of Magnetics 18(1), 21-25 (2013) http://dx.doi.org/10.4283/JMAG.2013.18.1.021

Crystallographic and Magnetic Properties of Nickel Substituted Manganese Ferrites Synthesized by Sol-gel Method

Kwang Pyo Chae*, Won Oak Choi, Jae-Gwang Lee, Byung-Sub Kang, and Seung Han Choi[1]

Nanotechnology Research Center, Department of Nano Science and Mechanical Engineering, Konkuk University, Chungju 380-701, Korea
[1]Department of Oriental Biomedical Engineering, Daegu Haany University, Gyeongsan 712-715, Korea.

(Received 26 November 2012, Received in final form 2 January 2013, Accepted 2 January 2013)

Nickel substituted manganese ferrites, $Mn_{1-x}Ni_xFe_2O_4$ ($0.0 \le x \le 0.6$), were fabricated by sol-gel method. The effects of sintering and substitution on their crystallographic and magnetic properties were studied. X-ray diffractometry of $Mn_{0.6}Ni_{0.4}Fe_2O_4$ ferrite sintered above 523 K indicated a spinel structure; particles increased in size with hotter sintering. The Mössbauer spectrum of this ferrite sintered at 523 K could be fitted as a single quadrupole doublet, indicative of a superparamagnetic phase. Sintering at 573 K led to spectrum fitted as the superposition of two Zeeman sextets and a single quadrupole doublet, indicating both ferrimagnetic and paramagnetic phase. Sintering at 673 K and at 773 K led to spectra fitted as two Zeeman sextets due to a ferrimagnetic phase. The saturation magnetization and the coercivity of $Mn_{0.6}Ni_{0.4}Fe_2O_4$ ferrite sintered at 773 K were 53.05 emu/g and 142.08 Oe. In $Mn_{1-x}Ni_xFe_2O_4$ ($0.0 \le x \le 0.6$) ferrites, sintering of any composition at 773 K led to a single spinel structure. Increased Ni substitution decreased the ferrites' lattice constants and increased their particle sizes. The Mössbauer spectra could be fitted as the superposition of two Zeeman sextets due to the tetrahedral and the octahedral sites of the Fe^{3+} ions. The variations of saturation magnetization and coercivity with changing Ni content could be explained using the changes of particle size.

Keywords : Mn-Ni ferrite, sol-gel method, superparamagnetic phase, Mössbauer spectroscopy, coercivity, saturation magnetization

1. Introduction

Manganese ferrite, $MnFe_2O_4$, is widely used in microwave and magnetic recording. Its spinel configuration is based on a face-centered cubic lattice of oxygen ions with a unit cell consisting of 8 functional units of $(Mn_xFe_{1-x})[Mn_{1-x}Fe_{1+x}]O_4$, in which the metallic cations in parentheses occupy the tetrahedral A-sites and those in the square brackets occupy the octahedral B-sites; "x" is defined as an inversion parameter. Nickel ferrite, $NiFe_2O_4$, is an inverse spinel in which the tetrahedral A-sites are occupied by Fe^{3+} ions and the octahedral B-sites by Fe^{3+} and Ni^{2+} ions [1, 2]. The resistivity of Mn ferrite is much lower than that of Ni ferrite, which allows Mn-Ni-Co and Cu-Ni-Co-Mn ferrites to be used as thermistors [3, 4]. Sol-gel synthesis with cooler sintering allows the fabrication of finer grained powders. It can provide multi-component oxides of homogeneous composition and has been used to prepare many high-purity oxide powders, including some with spinel-type structures. The sol-gel synthesis of substituted manganese ferrite is generally difficult, and there are a few detailed studies of Ni substituted manganese ferrites [5, 6].

This work reports the sol-gel synthesis of Ni substituted Mn ferrite powders of $Mn_{1-x}Ni_xFe_2O_4$ ($0.0 \le x \le 0.6$). The effects of sintering and substitution on their crystallographic and magnetic properties were assessed by X-ray diffractometry (XRD), field emission scanning electron microscopy (FESEM), Mössbauer spectroscopy and vibrating sample magnetometry (VSM).

2. Experiment

$Mn_{1-x}Ni_xFe_2O_4$ ($0.0 \le x \le 0.6$) ferrites were prepared by sol-gel synthesis. Measured amounts of $Mn(NO_3)_2 \cdot H_2O$, $Ni(NO_3)_2 \cdot 6H_2O$ and $Fe(NO_3) \cdot 9H_2O$ were first dissolved in 2-methoxyethanol for 30~50 minutes using an ultrasonic cleaner. The solution was refluxed at 353 K for 12 h to

*Corresponding author: Tel: +82-43-840-3623
Fax: +82-43-851-4169, e-mail: kpchae@kku.ac.kr

obtain a gel and dried at 363 K in an oven for 24 h. The resulting dried powders were ground and sintered at various temperatures to determine the particles' growth. All sintering was under an N_2 atmosphere to prevent oxidation of the Mn^{2+}. A high initial N_2 gas flow was used to purge oxygen from the quartz sample tube and to drive gas from the dry powder. The purities of samples were analyzed by X-ray diffractometry using CuKα (1.54 Å) radiation. Surface microstructure was observed using FESEM at room temperature. Mössbauer spectra were recorded using a ^{57}Co source in constant acceleration mode to identify the ferrite powders' magnetic phases. The saturation magnetization and coercivity were determined by VSM.

3. Results and Discussion

3.1. Sintering effects on $Mn_{0.6}Ni_{0.4}Fe_2O_4$ ferrite

The X-ray diffraction patterns of $Mn_{0.6}Ni_{0.4}Fe_2O_4$ ferrite sintered at various temperatures are shown in Fig. 1. They show that sintering at 523 K led to any crystallization peaks but above 573 K led to all the peaks coincident with a typical spinel structure, and that sintering at 773 K led to a lattice constant of 8.434 Å. Hotter sintering led to a sharper major peak, indicating larger particles in the spinel powder and improved crystallization. Pure $MnFe_2O_4$ obtained by sol-gel synthesis can be formed at 523 K, and thoroughly crystallized at above 523 K [7]. These temperatures are much lower than those required by traditional ceramic methods and suggest that the cooler sintering required by sol-gel synthesis leads to larger particles comparable to those of powders obtained by ceramic and wet chemical methods. Particles' sizes were determined from the broadening of diffraction peaks using Scherrer's equation [8], $t = 0.9\lambda/(B\cos\Theta_B)$, where λ represents the X-ray wavelength, B is the half width of the (311) peak, and Θ_B is the angle of the (311) peak. The particles of $Mn_{0.6}Ni_{0.4}Fe_2O_4$ grew with hotter sintering: 14 nm (573 K), 16 nm (673 K), 29 nm (773 K). The larger

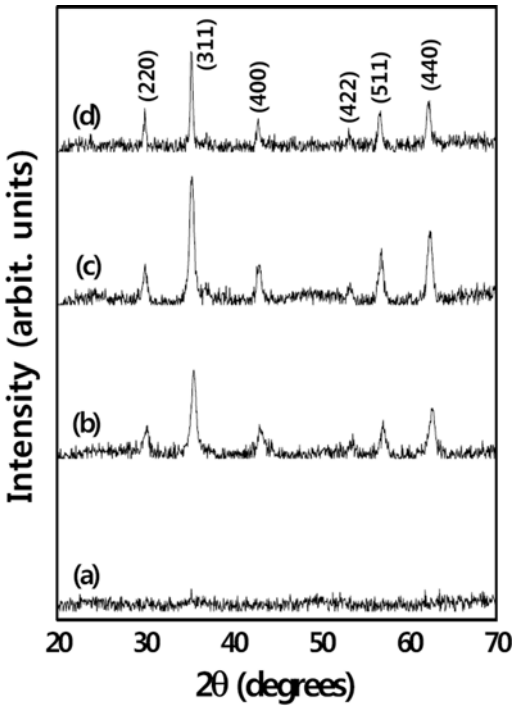

Fig. 1. X-ray diffraction patterns of $Mn_{0.6}Ni_{0.4}Fe_2O_4$ ferrite sintered at (a) 523 K, (b) 573 K, (c) 673 K and (d) 773 K.

particles obtained after hotter sintering were confirmed by FESEM photomicrographs taken under the same 100,000 magnification and at the same scale as shown in Fig. 2. The samples appear to consist of similar regular particles with a narrow size distribution. Hotter sintering led to more and bigger particles.

Mössbauer absorption spectra of the variously sintered $Mn_{0.6}Ni_{0.4}Fe_2O_4$ ferrite were measured at room temperature as shown in Fig. 3. Sintering at 523 K resulted in a spectrum was fitted with a single quadrupole doublet, indicating paramagnetism. Sintering at 573 K led to spectrum fitted with two sextets and one doublet, indicating that the ferrites had both ferrimagnetic and paramagnetic phases. Sintering at 673 K and at 773 K resulted in a spectra fitted with only two sextets, indicating ferrimagnetism.

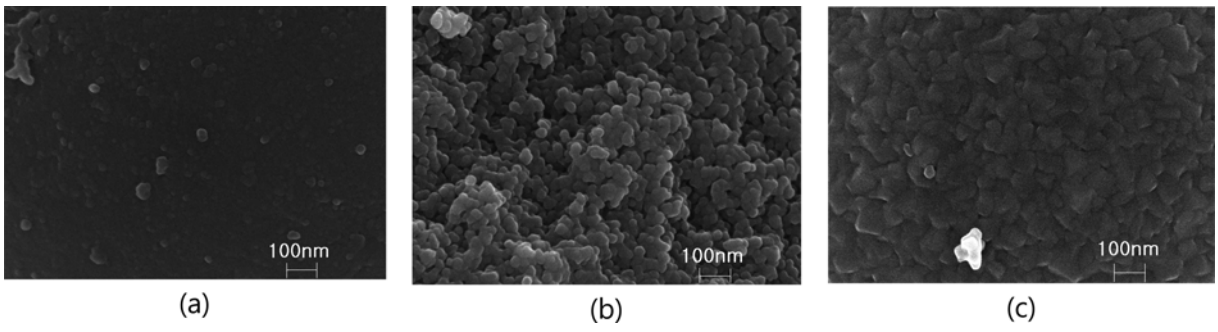

Fig. 2. FESEM images of $Mn_{0.6}Ni_{0.4}Fe_2O_4$ ferrite sintered at (a) 523 K, (b) 673 K and (c) 773 K.

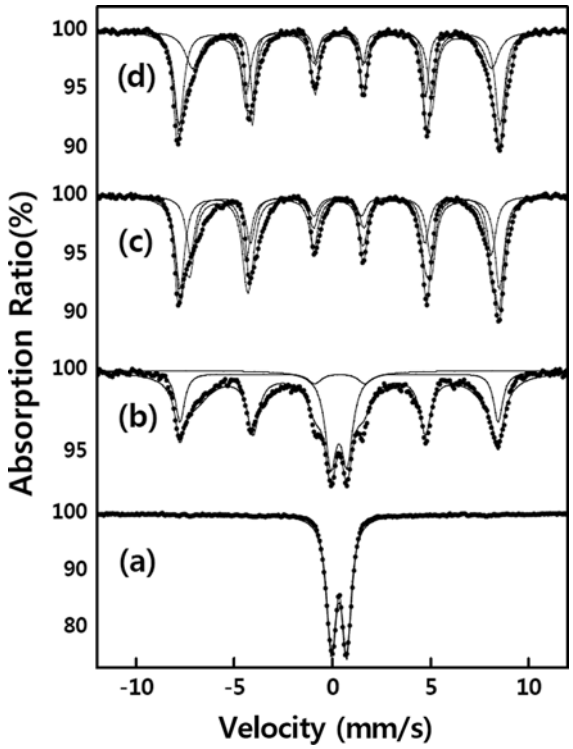

Fig. 3. Mössbauer spectra of $Mn_{0.6}Ni_{0.4}Fe_2O_4$ ferrite sintered at (a) 523 K, (b) 573 K, (c) 673 K and (c) 773 K.

The magnetic phase changes were due to the samples' different particle sizes. The superparamagnetism shown by the sample sintered at 523 K indicates particles are too small to maintain ferrimagnetism. Below the blocking temperature, T_B, the Mössbauer spectra show split magnetism. Above T_B, only paramagnetism is observed. The spectrum is broadened near T_B, where τ is close to the Mössbauer time of measurement τ_s (~10^{-8} s for ^{57}Fe Mössbauer spectroscopy). Above T_B, the relaxation time $\tau < \tau_s$ and only a quadruple doublet spectrum is observed. At $\tau > \tau_s$, a sextet Mössbauer pattern is observed, as shown by the low temperature Mössbauer spectra reported for $MnFe_2O_4$ [9].

The magnetic properties of the $Mn_{0.6}Ni_{0.4}Fe_2O_4$ ferrite were determined at room temperature by vibrating sample magnetometry. Hysteresis curves in the maximal field of 6 kOe were recorded for the variously sintered samples as shown in Fig. 4. Coercivity was increased as the sintering temperature rose above 523 K. Saturation magnetization was also increased greatly with hotter sintering. Sintering at 523 K led to low coercivity and saturation magnetization due to the superparamagnetic phase of the ferrite particles which were mostly smaller than the critical size necessary for ferrimagnetism, as confirmed by the Mössbauer spectrum. Similar results have been reported for nanoparticles of $Ni_{0.9}Zn_{0.1}Fe_2O_4$ [10]. The $Mn_{0.6}Ni_{0.4}Fe_2O_4$ ferrite showed

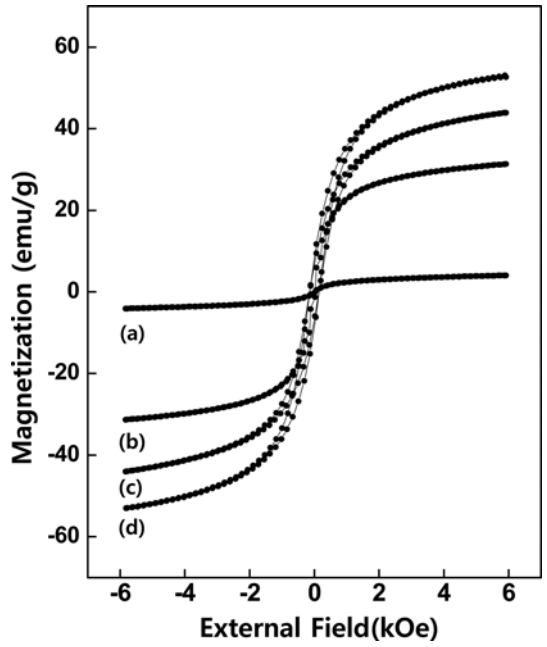

Fig. 4. Hysteresis curves of $Mn_{0.6}Ni_{0.4}Fe_2O_4$ ferrite sintered at (a) 523 K, (b) 573 K, (c) 673 K and (d) 773 K.

greatest saturation magnetization and coercivity (53.05 emu/g and 142.08 Oe, respectively) after sintering at 773 K. The observed values were greater than those of pure $MnFe_2O_4$ ferrite (42.83 emu/g and 79.15 Oe).

3.2. Nickel substitution effects on manganese ferrite

The X-ray diffraction patterns of the $Mn_{1-x}Ni_xFe_2O_4$

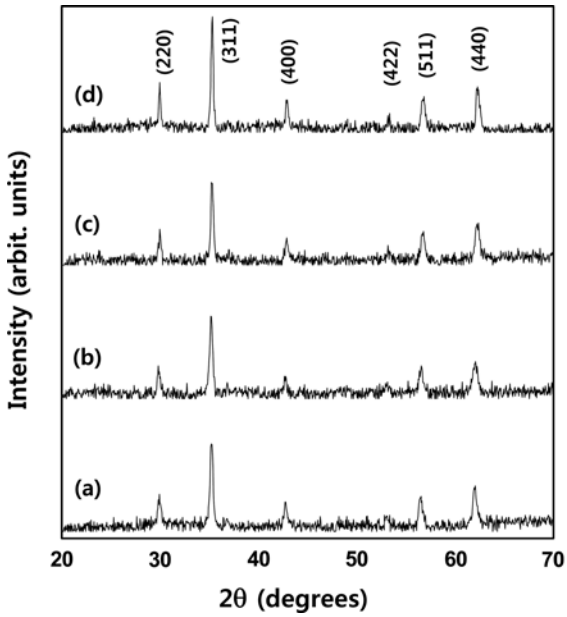

Fig. 5. X-ray diffraction patterns of $Mn_{1-x}Ni_xFe_2O_4$ ferrites sintered at 773 K: (a) x = 0.0, (b) x = 0.2, (c) x = 0.4 and (d) x = 0.6.

($0.0 \leq x \leq 0.6$) ferrites sintered at 773 K indicate typical spinel structures as shown in Fig. 5. Increasing Ni content led to a linear decrease of the ferrites' lattice constants as 8.475 Å (x = 0.0), 8.437 Å (x = 0.2), 8.414 Å (x = 0.4) and 8.341 Å (x = 0.6). This could be explained on the basis of Vegard's law regarding the differences in the ionic radii of Mn^{2+} ions (0.91 Å) and Ni^{2+} ions (0.72 Å). The particle size of $Mn_{1-x}Ni_xFe_2O_4$ grew with Ni substitution increased: 25 nm (x = 0.0), 26 nm (x = 0.2), 29 nm (x = 0.4) and 34 nm (x = 0.6). The larger particles obtained after Ni substitution were confirmed by FESEM images of the samples with x = 0.0 and 0.6, both sintered at 773 K, were recorded under the same 100,000 magnifications and at the same scale as shown in Fig. 6. They show that increased Ni substitution increased the particles' size.

Sintering at 773 K consistently led to get Mössbauer absorption spectra that could be fitted as the superposition of two Zeeman sextets assigned to the tetrahedral and octahedral sites of the Fe^{3+} ions [10]. The Mössbauer parameters of the samples' tetrahedral sites varied with Ni content as shown in Fig. 7: H_{hf} is the magnetic hyperfine field, *QS* is the quadrupole splitting, and *IS* represents the isomer shift relative to metallic iron. H_{hf} values were increased slightly with increased Ni substitution. The samples' constant *QS* values indicate that the electric field gradient was unchanged by the Ni substitution. *IS* values were slightly increased with increasing Ni substitution.

Cation distribution depends on many factors such as temperature, pressure and composition [11, 12], and also the preparation method [13, 14]. Using an occupation preference of Ni ions for B-sites in a spinel structure, the cation distributions in the samples sintered at 773 K were determined from the Mössbauer spectra:

$(Mn_{0.52}Fe_{0.48})[Mn_{0.48}Fe_{1.52}]O_4$ for x = 0.0,
$(Mn_{0.40}Fe_{0.60})[Mn_{0.40}Ni_{0.2}Fe_{1.40}]O_4$ for x = 0.2,
$(Mn_{0.28}Fe_{0.72})[Mn_{0.32}Ni_{0.4}Fe_{1.28}]O_4$ for x = 0.4,
$(Mn_{0.12}Fe_{0.88})[Mn_{0.28}Ni_{0.6}Fe_{1.12}]O_4$ for x = 0.6.

The ferrites' magnetic properties were determined at room temperature using a vibrating sample magnetometer in a maximal field of 6 kOe. The hysteresis curves revealed a typical soft ferrite pattern. Saturation magnetization and coercivity increased with increasing Ni concentration as shown in Table 1. The changes can be explained by considering the different site distributions and spin magnetic moments of the substituted ions. The Mössbauer absorption

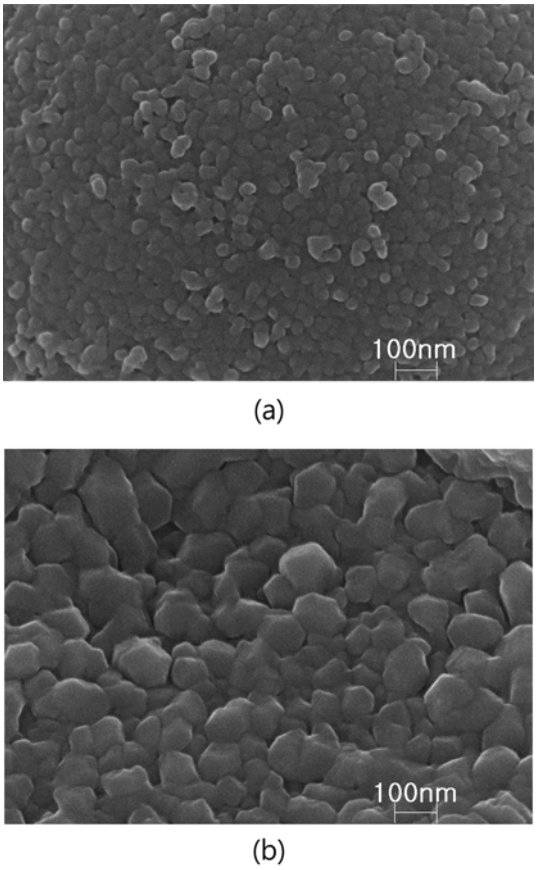

Fig. 6. FESEM images of $Mn_{1-x}Ni_xFe_2O_4$ ferrites sintered at 773 K: (a) x = 0.0 and (b) x = 0.6.

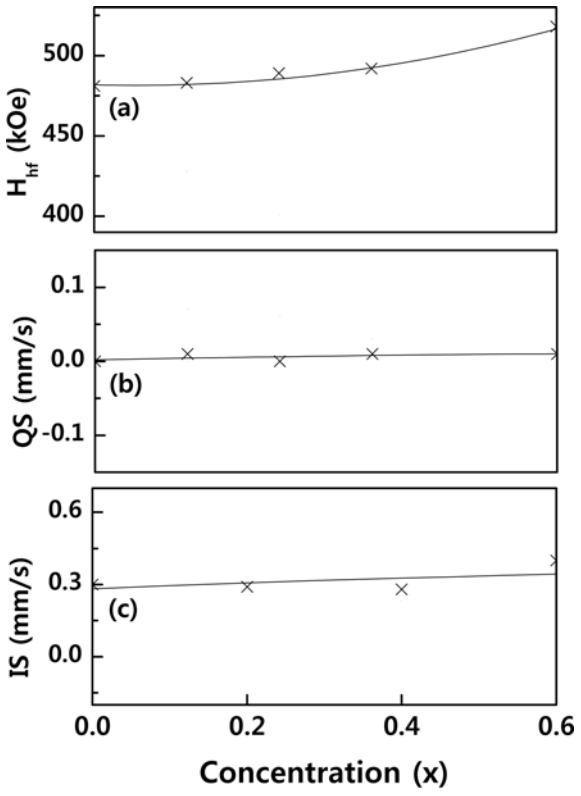

Fig. 7. Variation of Mössbauer parameters of tetrahedral site in $Mn_{1-x}Ni_xFe_2O_4$ ferrites sintered at 773 K: (a) hyperfine field, (b) quadrupole splitting and (c) isomer shift.

Table 1. Saturation magnetization (M_s) and coercivity (H_c) of $Mn_{1-x}Ni_xFe_2O_4$ ferrites sintered at 773 K.

Samples (x)	M_s (emu/g)	H_c (Oe)
0.0	42.83	79.15
0.2	45.68	119.40
0.4	53.05	142.08
0.6	61.20	146.25

area showed that the octahedral Mn and Fe ions decreased and the Ni ions increased up to x = 0.6. The substitution of ions with greater magnetic moments (Mn $^{2+}$ and Fe^{3+} = 5 μ_B) by those with a lesser magnetic moment (Ni^{2+} = 2 μ_B) could be expected to lower the saturation magnetization: such was observed by K. J. Kim in Mn-Co thin film [15]. However, the results of this work do not support this explanation. Therefore, it may be concluded that the Ni ion substitution effects on the saturation magnetization and the coercivity was not as greatly as the particles' sizes. The XRD and FESEM results show that the particles increased in size with increasing Ni ion substitution, which could have led to the increased saturation magnetization and coercivity. Similar has been reported of $Co_{0.5}Mn_{0.5}Fe_2O_4$ nanoparticles [16]. The maximum saturation magnetization and coercivity of $Mn_{1-x}Ni_xFe_2O_4$ ($0.0 \leq x \leq 0.6$) were 61.20 emu/g and 146.25 Oe, respectively, at x = 0.6.

4. Conclusion

Ni substituted manganese ferrite, $Mn_{0.6}Ni_{0.4}Fe_2O_4$, had a single spinel structure when sintered above 523 K. Its constituent particles increased in size with hotter sintering. The Mössbauer spectrum of $Mn_{0.6}Ni_{0.4}Fe_2O_4$ ferrite sintered at 523 K could be fitted as a doublet, indicating a superparamagnetic phase. Sintering at 673 K and at 773 K led to spectra could be fitted as two Zeeman sextets, indicating a ferrimagnetic phase. Sintering at 573 K led to spectrum could be fitted as a superposition of two Zeeman sextets and a single quadrupole doublet, indicating both ferrimagnetic and paramagnetic phases.

$Mn_{1-x}Ni_xFe_2O_4$ ($0.0 \leq x \leq 0.6$) ferrites sintered at 773 K showed a single spinel structure. Their lattice constants decreased but particles size increased with increasing substitution of Ni. Their Mössbauer spectra could be fitted as the superposition of two Zeeman sextets due to the tetrahedral and octahedral sites of the Fe^{3+} ions. The samples' hysteresis curves consistently show a typical soft ferrite pattern. The variations of saturation magnetization and coercivity with changing Ni content could be explained using the changes of particle size. The $Mn_{1-x}Ni_xFe_2O_4$ ferrites achieved a maximum saturation magnetization and coercivity of 61.20 emu/g and 146.25 Oe, respectively, at x = 0.6.

Acknowledgements

This paper was supported by Konkuk University in 2012.

References

[1] A. S. Albaguergye, J. D. Ardisson, and W. A. A. Macedo, J. Appl. Phys. **87**, 4352 (2000).
[2] A. Goldman, Modern Ferrite Technology, Van Nostrand Reinhold, New York (1990), p. 217.
[3] P. A. Shaikh, R. C. Kamble, A. V. Rao, and Y. D. Kolekar, J. Alloys Compd. **492**, 590 (2010).
[4] D. A. Kukuruznyak, J. G. Mayer, N. T. Nguyen, E. A. Stern, and F. S. Ohuchi, J. Electro. Spectro. Relatd Pheno. **150**, 275 (2006).
[5] W. H. Kwon, J. Y. Kang, J. G. Lee, S. W. Lee, and K. P. Chae, J. Magnetics **15**, 159 (2010).
[6] S. W. Lee, J. G. Lee, K. P. Chae, W. H. Kwon, and C. S. Kim, J. Kor. Mag. Soc. **19**, 57 (2009).
[7] B. D. Cullity, Elements of X-Ray Diffraction, Addition-Wesley Co. Readings, MA (1978), p. 102.
[8] S. W. Lee and C. S. Kim, J. Magn. Magn. Mater. **304**, 418 (2006).
[9] S. W. Lee and C. S. Kim, J. Magnetics **10**, 5 (2005).
[10] W. H. Kwon, Ph.D. thesis, Konkuk University (2010) p. 98.
[11] M. Z. Schmalzrifd. J. Phys. Chem. **28**, 203 (1961).
[12] R. K. Datta and B. Roy, J. Amer. Coram. Soc. **50**, 578 (1967).
[13] N. Yamamoto, S. Kawano, N. Achwa, M. Kiyama, and T. Takada, Japan. J. Appl. Phys. **12**, 1830 (1973).
[14] A. Meenasmsrndaram, N. Gunasekaran, and V. Sninivasan, Phys. Stat. Sol. (A) **69**, K45 (1982).
[15] K. J. Kim, H. K. Kim, Y. R. Park, and J. Y. Park, J. Kor. Mag. Soc. **16**, 23 (2006).
[16] M. K. Shobana, S. Sankar, and V. Rayendran, Mater. Chem. Phys. **113**, 10 (2009).